Chapter 1

Spatial beam structures

1.1 Beam axis and cross section definition

A basic necessary condition for identifying a deformable body as a beam – and hence applying the associated framework – is that its centroidal curve be at least loosely recognizable.

Once such centroidal line has been roughly defined, locally perpendicular planes may be derived whose intersection with the body itself defines the local beam cross section.

Then, the G center of gravity position may be computed for each of the local cross sections, leading to a refined, potentially iterative definition for the beam centroidal axis[1].

A local cross-sectional reference system may be defined by aligning the normal z axis with the beam centroidal curve, and by employing, as the first in-section axis, namely x, the projection of a given global $\underline{\mathrm{v}}$ vector, which is assumed not to be parallel to the beam axis.

The second in-section axis y may be then derived, in order to obtain a $Gxyz$ right-handed coordinate system, whose unit vectors are $\hat{\imath}, \hat{\jmath}, \hat{k}$.

If a thin walled profile is considered in place of a solid cross section member – i.e., the section wall midplane is recognizable too (see paragraph XXX), then a curvilinear coordinate $0 \leq s \leq l$ may be defined that spans the in-cross-section wall midplane, along with a local through-wall-thickness coordinate $-t(s)/2 \leq r \leq +t(s)/2$.

Such s, r, in-section coordinates based on the profile wall may be employed in place of their cartesian x, y counterparts, if favourable.

Beam axis may be discontinuous at sudden body geometry changes; a rigid body connection is ideally assumed to restrict the relative motion of the proximal segments. Such rigid joint modeling may be extended to more complex n-way joints; if the joint finite stiffness is to be taken into account, it has to be described through the entries of a rank $6(n-1)$ symmetric square matrix [2].

At joints or beam axis angular points the cylindrical bodies swept by the cross sections do usually overlap, besides they only loosely mimic the actual deformable body geometry; the results obtained through the local application of the elementary beam theory may at most be

[1] Here, centroidal curve, centroidal line, centroidal axis, or simply beam axis are treated as synonyms.

[2] i.e., joint stiffness is unfortunately not a scalar value.

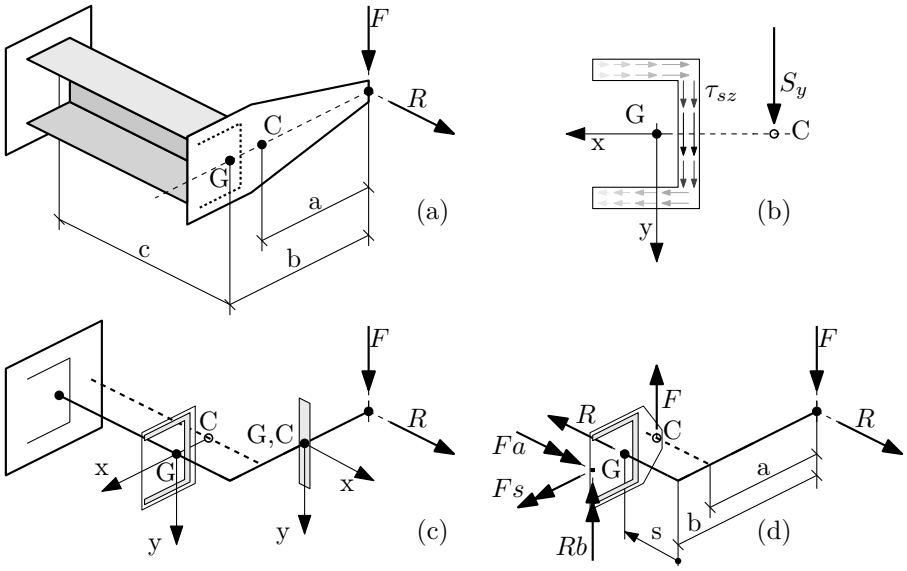

Figure 1.1: A beam structure.

employed to scale the triaxial local stress/strain fields[3], which have to be evaluated resorting to more complex modelings.

1.1.1 A worked example

See Figure 1.1. TODO.

1.2 Cross-sectional resultants for the spatial beam

At any point along the axis the beam may be notionally split, thus obtaining two facing cross sections, whose interaction is limited to three components of interfacial stresses, namely the axial normal stress σ_{zz} and the two shear components τ_{yz}, τ_{zx}.

Three force resultant components may be defined by integration along the cross section area, namely the normal force, the y- and the

[3]The peak stress values obtained through the elementary beam theory may be profitably employed as *nominal stresses* within the stress concentration effect framework.

x- oriented shear forces, respectively defined as

$$N = \int_{\mathcal{A}} \sigma_{zz} d\mathcal{A}$$
$$S_y = \int_{\mathcal{A}} \tau_{yz} d\mathcal{A}$$
$$S_x = \int_{\mathcal{A}} \tau_{zx} d\mathcal{A}$$

Three moment resultant components may be similarly defined, namely the x- and y- oriented bending moments, and the torsional moment. However, if the centroid is the preferred fulcrum for evaluating the bending moments, the below discussed C shear center is employed for evaluating the torsional moment. We hence define

$$\mathcal{M}_x = \int_{\mathcal{A}} \sigma_{zz} y d\mathcal{A}$$
$$\mathcal{M}_y = -\int_{\mathcal{A}} \sigma_{zz} x d\mathcal{A}$$
$$\mathcal{M}_t \equiv \mathcal{M}_z = \int_{\mathcal{A}} \left[\tau_{yz}(x - x_C) - \tau_{zx}(y - y_C)\right] d\mathcal{A}$$

The applied vector associated to the normal force component $(G, N\hat{k})$ is located at the section center of gravity , whereas the shear force $(C, S_x\hat{\imath} + S_y\hat{\jmath})$ is supposed to act at the shear center; such convention decouples the energy contribution of force and moment components for the straight beam.

Cross section resultants may be obtained, based on equilibrium for a statically determinate structure. The ordinary procedure consists in

- notionally splitting the structure at the cross section whose resultants are under scrutiny;
- isolating a portion of the structure that ends at the cut, whose locally applied loads are all known; the structure has to be preliminarily solved for the all the constraint reactions that act on the isolated portion;
- setting the equilibrium equations for the isolated substructure, according to which the cross-sectional resultants are in equilibrium with whole loading.

1.3 Axial load and uniform bending

It is preliminarily noted that the elementary extensional-flexural solution is exact with respect to the Theory of Elasticity if the following conditions hold:

- beam constant section;
- beam rectilinear axis;
- absence of locally applied loads;
- absence of shear resultants[4] (i.e. constant bending moments);
- principal material directions of orthotropy are uniform along the section, and one of them is aligned with the beam axis;
- the ν_{31} and the ν_{32} Poisson's ratios[5] are constant along the section, where 3 means the principal direction of orthotropy aligned with the axis. Please note that $E_i\nu_{ji} = E_j\nu_{ij}$, and hence $\nu_{ji} \neq \nu_{ij}$ for a generally orthotropic material.

Most of the above conditions are in fact violated in many textbook structural calculations, thus suggesting that the elementary beam theory is robust enough to be adapted to practical applications, i.e. limited error is expected if some laxity is used in circumscribing its scope[6].

The extensional-flexural solution builds on the basis of the following simplifying assumptions:

- the in-plane[7] stress components $\sigma_x, \sigma_y, \tau_{xy}$ are null;
- the out-of-plane shear stresses τ_{yz}, τ_{zx} are also null;

[4] A locally pure shear solution may be in fact superposed; such solution may however not be available for a general cross section.

[5] We recall that ν_{ij} is the Poisson's ratio that corresponds to a contraction in direction j, being a unitary extension applied in direction i in a manner that the elastic body is subject to a uniaxial stress state.

[6] Measures for both the error and the violation have to be supplied first in order to quantify the approximation.

[7] Both the *in-plane* and the *out-of-plane* expressions for the characterization of the stress/strain components refer to the cross sectional plane.

- the axial elongation ϵ_z linearly varies along the cross section, namely
$$\epsilon_z = a + bx + cy \tag{1.1}$$
or, equivalently[8], each cross section is assumed to remain planar in the deformed configuration.

The three general constants a, b and c possess a physical meaning; in particular a represents the axial elongation $\bar{\epsilon}$ as measured at the centroid[9], c represents the $1/\rho_x$ curvature[10] whereas b represent the $1/\rho_y$ curvature, apart from its sign.

Figure 1.2 (c) justifies the equality relation $c = 1/\rho_x$; the beam axial fibers with a Δz initial length are elongated by the curvature up to a $\Delta\theta\,(\rho_x + y)$ deformed length, where $\Delta\theta\rho_x$ equates Δz based on the length of the unextended fibre at the centroid. By evaluating the axial strain value for a general fiber, it follows that $\epsilon_z = 1/\rho_x\, y$.

In addition, Figure 1.2 (c) relates the $1/\rho_x$ curvature to the displacement component in the local y direction, namely v, and to the section rotation angle with respect to the local x axis, namely θ, thus obtaining
$$\frac{d\theta}{dz} = \frac{1}{\rho_x}, \quad \theta = -\frac{dv}{dz}, \quad \frac{d^2v}{dz^2} = -\frac{1}{\rho_x} \tag{1.2}$$

Following analogous considerations, see 1.2 (e), we may similarly obtain
$$\frac{d\phi}{dz} = \frac{1}{\rho_y}, \quad \phi = +\frac{du}{dz}, \quad \frac{d^2u}{dz^2} = +\frac{1}{\rho_y} \tag{1.3}$$
where ϕ is the cross section rotation about the local y axis, and u is the x displacement component.

According to the assumptions in the preamble, a uniaxial stress state is assumed, where the only nonzero σ_z stress component may be determined as
$$\sigma_z = E_z\epsilon_z = E_z\left(\bar{\epsilon} - \frac{1}{\rho_y}x + \frac{1}{\rho_x}y\right) \tag{1.4}$$

[8]The axial, out-of-plane displacement $\Delta w = \int_{\Delta l}\epsilon_z dz = \Delta_l\,(a + bx + cy)$ accumulated between two contiguous cross sections with an Δl initial distance, is consistent with that of a relative rigid body motion.

[9]or, equivalently, the average elongation along the section, in an integral sense.

[10]namely the inverse of the beam curvature radii as observed with a line of sight aligned with the x axis. Curvature is assumed positive if the associated θ section rotation grows with increasing z, i.e. $d\theta/dz > 0$.

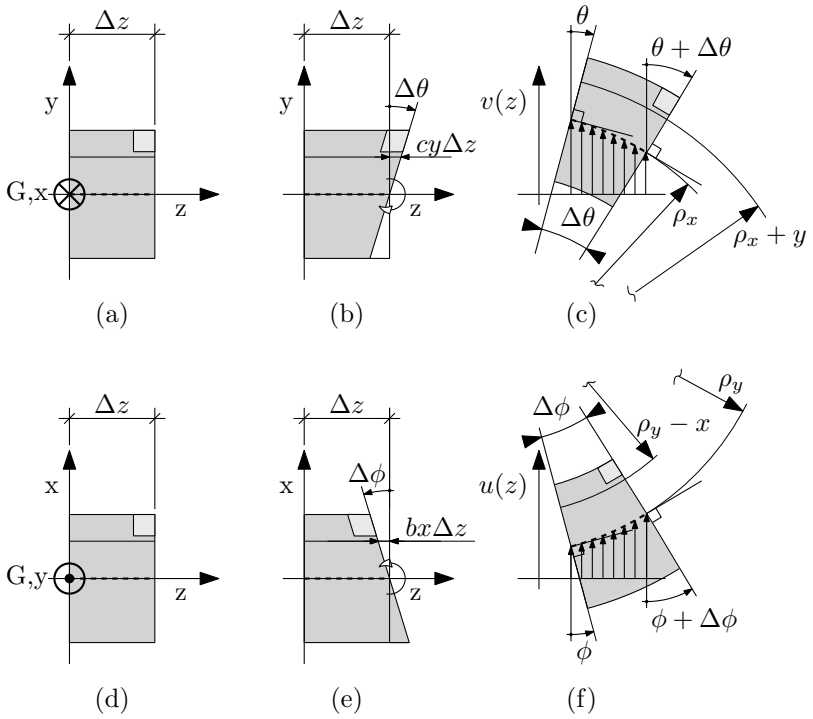

Figure 1.2: A differential fibre elongation proportional to the y coordinate induces a curvature $1/\rho_x$ on the normal plane with respect to the x axis. A differential fibre contraction proportional to the x coordinate induces a curvature $1/\rho_y$ on the normal plane with respect to the y axis. The didascalic trapezoidal deformation modes (b) and (e) clearly associate the differential elongation/contraction with the positive relative end rotation; they are however affected by a spurious shear deformation as evidenced by the skewed corner.

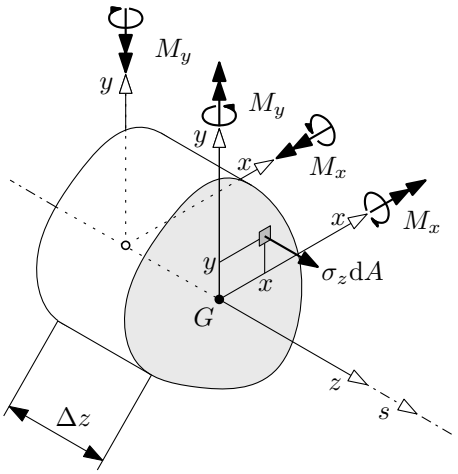

Figure 1.3: Positive x and y bending moment components adopt the same direction of the associated local axes at the beam segment end showing an outward-oriented arclength coordinate axis; at beam segment ends characterized by an inward-oriented local z axis, the same positive bending moment components are locally counter-oriented to the respective axes.

Stress resultants may easily be evaluated based on Fig. 1.3 as

$$N = \iint_{\mathcal{A}} E_z \epsilon_z dA = \overline{EA}\bar{\epsilon} \tag{1.5}$$

$$\mathcal{M}_x = \iint_{\mathcal{A}} E_z \epsilon_z y dA = \overline{EJ}_{xx} \frac{1}{\rho_x} - \overline{EJ}_{xy} \frac{1}{\rho_y} \tag{1.6}$$

$$\mathcal{M}_y = -\iint_{\mathcal{A}} E_z \epsilon_z x dA = -\overline{EJ}_{xy} \frac{1}{\rho_x} + \overline{EJ}_{yy} \frac{1}{\rho_y} \tag{1.7}$$

where the combined material/cross-section stiffness moduli

$$\overline{EA} = \iint_{\mathcal{A}} E_z(x,y)\, dA \tag{1.8}$$

$$\overline{EJ}_{xx} = \iint_{\mathcal{A}} E_z(x,y) yy\, dA \tag{1.9}$$

$$\overline{EJ}_{xy} = \iint_{\mathcal{A}} E_z(x,y) yx\, dA \tag{1.10}$$

$$\overline{EJ}_{yy} = \iint_{\mathcal{A}} E_z(x,y) xx\, dA \tag{1.11}$$

may also be rationalized as the cross section area and moment of inertia, respectively, multiplied by a suitably averaged Young modulus, evaluated in the axial direction.

Those moduli simplify to their usual $E_z A, E_z J_{**}$ analogues, where the influence of the material and of the geometry are separated if the former is homogeneous along the beam cross section.

From Eqn. 1.5 we obtain

$$\bar{\epsilon} = \frac{N}{\overline{EA}}. \tag{1.12}$$

By concurrently solving Eqns. 1.6 and 1.7 with respect to the $1/\rho_x$ and $1/\rho_y$ curvatures, we obtain

$$\frac{1}{\rho_x} = \frac{\mathcal{M}_x \overline{EJ}_{yy} + \mathcal{M}_y \overline{EJ}_{xy}}{\overline{EJ}_{xx}\overline{EJ}_{yy} - \overline{EJ}_{xy}^2} \tag{1.13}$$

$$\frac{1}{\rho_y} = \frac{\mathcal{M}_x \overline{EJ}_{xy} + \mathcal{M}_y \overline{EJ}_{xx}}{\overline{EJ}_{xx}\overline{EJ}_{yy} - \overline{EJ}_{xy}^2} \tag{1.14}$$

Axial strain and stress components may then be obtained for any cross section point by substituting the above calculated generalized strain components $\bar{\epsilon}$, $1/\rho_x$ and $1/\rho_y$ holding for the extensional-flexural beam into Eqn. 1.4, thus obtaining

$$\sigma_z = E_z \epsilon_z \tag{1.15}$$

$$= \alpha \mathcal{M}_x + \beta \mathcal{M}_y + \gamma N \tag{1.16}$$

where

$$\alpha\left(x, y, E_z, \overline{EJ}_{**}\right) = E_z(x, y)\frac{-\overline{EJ}_{xy}x + \overline{EJ}_{yy}y}{\overline{EJ}_{xx}\overline{EJ}_{yy} - \overline{EJ}_{xy}^2} \tag{1.17}$$

$$\beta\left(x, y, E_z, \overline{EJ}_{**}\right) = E_z(x, y)\frac{-\overline{EJ}_{xx}x + \overline{EJ}_{xy}y}{\overline{EJ}_{xx}\overline{EJ}_{yy} - \overline{EJ}_{xy}^2} \tag{1.18}$$

$$\gamma\left(x, y, E_z, \overline{EA}\right) = E_z(x, y)\frac{1}{\overline{EA}}. \tag{1.19}$$

The peak axial strain is obtained at points farther from neutral axis of the stretched section; such neutral axis may be graphically defined as follows:

- the coordinate pair

  $$(x_N, y_N) \equiv \left(\frac{\bar{e}\rho_x^2\rho_y}{\rho_x^2 + \rho_y^2}, -\frac{\bar{e}\rho_x\rho_y^2}{\rho_x^2 + \rho_y^2}\right);$$

  defines its nearest pass-through point with respect to the G centroid; the two points coincide in the case $\bar{\epsilon} = 0$.

- its orientation is defined by the unit vector

  $$\hat{n}_\parallel = \sqrt{\rho_x^2 + \rho_y^2}\left(\frac{1}{\rho_x}, \frac{1}{\rho_y}\right),$$

  whereas the direction

  $$\hat{n}_\perp = \sqrt{\rho_x^2 + \rho_y^2}\left(-\frac{1}{\rho_y}, \frac{1}{\rho_x}\right),$$

  is orthogonal to the neutral axis, and oriented towards growing axial elongations.

The cross section projection on the $(N, \hat{n}_\perp)$ line defines a segment whose ends are extremal with respect to the axial strain.

If the bending moment and the curvature component vectors are imposed to be parallel, i.e.

$$\lambda\begin{bmatrix}\mathcal{M}_x\\ \mathcal{M}_y\end{bmatrix} = \begin{bmatrix}\frac{1}{\rho_x}\\ \frac{1}{\rho_y}\end{bmatrix} = \underbrace{\frac{1}{\overline{EJ}_{xx}\overline{EJ}_{yy} - \overline{EJ}_{xy}^2}\begin{bmatrix}\overline{EJ}_{yy} & \overline{EJ}_{xy}\\ \overline{EJ}_{xy} & \overline{EJ}_{xx}\end{bmatrix}}_{[\overline{EJ}]}\begin{bmatrix}\mathcal{M}_x\\ \mathcal{M}_y\end{bmatrix} \tag{1.20}$$

an eigenpair problem is defined that leads to the definition of the principal directions for the cross sectional bending stiffness. In particolar, the eigenvectors of the $[\overline{EJ}]$ matrix define the two principal bending stiffness directions, and the associated $\overline{EJ}_{11}, \overline{EJ}_{22}$ eigenvalues constitute the associated bending stiffness moduli.

TODO: please elaborate...

1.4 Stresses due to the shear cross section resultants

In the presence of nonzero shear resultants, the bending moment exhibits a linear variation with the axial coordinate z in a straight beam. Based on the beam segment equilibrium we have

$$S_y = \frac{d\mathcal{M}_x}{dz}, \quad S_x = -\frac{d\mathcal{M}_y}{dz}, \tag{1.21}$$

as rationalized in Fig. XXX (a), with $\Delta z \to 0$ and $\mathcal{M}_x, \mathcal{M}_y$ differentiable with respect to z.

The linear variation of the bending-induced curvature in z causes a likewise linear variation of the pointwise axial strain; stress variation is also linear in the case of constant E_z longitudinal elastic modulus.

In particular, the differentiation with respect to z of σ_z as espressed in Eqn. 1.16 returns

$$\frac{d\sigma_z}{dz} = \alpha\left(x, y, E_z, \overline{EJ}_{**}\right) S_y - \beta\left(x, y, E_z, \overline{EJ}_{**}\right) S_x \tag{1.22}$$

since its α, β, γ factors are constant with respect to z; the bending moment derivatives are here expressed in terms of the shear resultants, as in Eqns. 1.21.

Figure 1.4 rationalizes the axial equilibrium for an elementary volume of material; we have

$$\frac{d\tau_{zx}}{dx} + \frac{d\tau_{yz}}{dy} + \frac{d\sigma_z}{dz} + q_z = 0 \tag{1.23}$$

where, for the specific case, the distributed volumetric load q_z is zero.

It clearly emerges from such relation that the shear stresses τ_{zx}, τ_{yz}, that were null within the uniform bending framework, are non-uniform along the section – and hence not constantly zero – in the presence of shear resultants.

A treatise on the pointwise solution of a) the equilibrium equations 1.23, once coupled with b) the compatibility conditions and with c) the the material elastic response, is beyond the scope of the present contribution, although it has been derived for selected cross sections in e.g. [1].

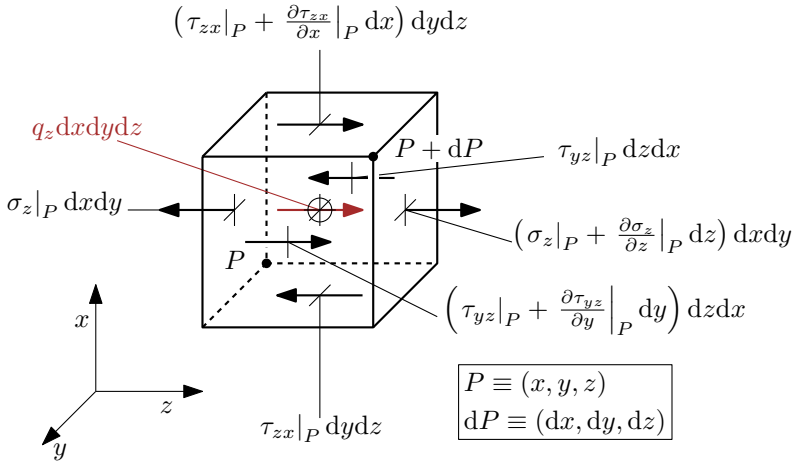

Figure 1.4: Equilibrium conditions with respect to the axial z translation for the infinitesimal volume extracted from the beam. In the case under scrutiny, the distributed volume action q_z is null.

1.4.1 The Jourawsky approach and its extension for a general section

The aforementioned axial equilibrium condition, whose treatise is cumbersome for the infinitesimal volume, may be more conveniently dealt with if a finite portion of the beam segment is taken into account, as in Figure 1.5.

A beam segment is considered whose axial extent is dz; the beam cross section is partitioned based on a (possibly curve, see Fig. 1.4.1) line that isolates an area portion A^* – and the related beam segment portion – for further scrutiny; axial equilibrium equation may then be stated for the isolated beam segment portion as follows

$$\bar{\tau}_{zi} t = \int_{A^*} \frac{d\sigma_z}{dz} dA, \tag{1.24}$$

where

$$\bar{\tau}_{zi} = \frac{1}{t} \int_t \tau_{zi} dr \tag{1.25}$$

is the average shear stress acting in the z direction along the cutting surface; i is the (locally normal) inward direction with respect to such

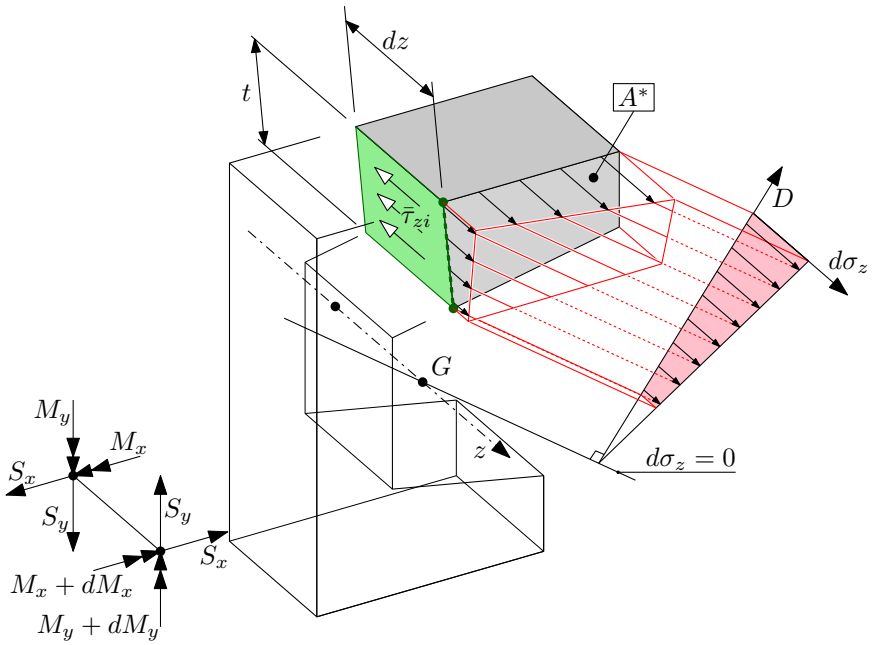

Figure 1.5: Equilibrium conditions for the isolated beam segment portion. It is noted that the null σ_z variation locus, $d\sigma_z = 0$, does not coincide with the bending neutral axis in general. Also, the depicted linear variation of $d\sigma_z$ with the D distance from such null $d\sigma_z$ locus does not hold in the case of non-uniform E_z modulus.

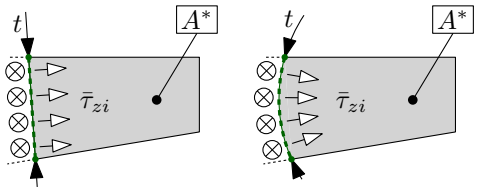

Figure 1.6: The curve employed for isolating the beam segment portion defines the direction of the τ_{zi} components whose average value is evaluated.

a surface. Due to the reciprocal nature of the shear stresses, the same $\bar{\tau}_{zi}$ shear stress acts along the cross sectional plane, and locally at the cutting curve itself. These shear actions are assumed positive if inward directed with respect to A^*.

The $\bar{\tau}_{zi}t$ product is named *shear flow*, and may be evaluated along a general cutting curve.

It is noted that, according to Eqn. 1.24, no information is provided with regard to a) the τ_{zt} shear stress that acts parallel to the cutting curve, nor b) the pointwise variation of τ_{zi} with respect of its average value $\bar{\tau}_{zi}$. If the resorting to more cumbersome calculation frameworks is not an option, those quantities are usually just neglected; an informed choice for the cutting curve is thus critical for a reliable application of the method.

In the simplified case of a) uniform material and b) local x, y axes that are principal axes of inertia (i.e. $J_{xy} = 0$), the usual formula is obtained

$$\bar{\tau}_{zi}t = \int_{A^*} \left(\frac{yS_y}{J_{xx}} + \frac{xS_x}{J_{yy}} \right) dA = \frac{\bar{y}^* A^*}{J_{xx}} S_y + \frac{\bar{x}^* A^*}{J_{yy}} S_x, \tag{1.26}$$

where $\bar{y}^* A^*$ and $\bar{x}^* A^*$ are the first order area moments of the A^* section portion with respect to the x and y axes, respectively[11].

1.4.2 Shear induced stresses in an open section, thin walled beam

In the case of thin walled profiles, the integral along the isolated area in Eqn. 1.24 may be performed with respect to the arclength coordinate alone; the value the $d\sigma_z/dz$ integrand assumes at the wall midplane is supposed representative of its integral average along the wall thickness, thus obtaining

$$\bar{\tau}_{zi}t = \int_0^s \frac{d\sigma_z}{dz} t d\varsigma. \tag{1.27}$$

Such assumed equivalence strictly holds for a) straight wall segments[12] and b) a linear variation of the integrand along the wall, a

[11] According to the employed notation, $(\bar{x}^*, \bar{y}^*)$ are the centre of gravity coordinates for the A^* area.

[12] i.e. the Jacobian of the $(s, r) \mapsto (x, y)$ mapping is constant with r.

condition, the latter, that holds if the material properties are homogeneous with respect to the wall midplane[13]; in the more general case, the error incurred by this approach vanishes with vanishing thickness for what concerns assumption a), whereas an average $\bar{E}_z$ modulus may be employed in place of the pointwise E_z midplane value if the material is inhomogeneous.

If a thin walled section segment is considered such that it is not possible to infer that the interfacial shear stress is zero at at least one of its extremities, a further term needs to be considered for the equilibrium, thus obtaining

$$\bar{\tau}_{zi}(s)t(s) = \int_a^s \frac{d\sigma_z}{dz} t d\varsigma + \bar{\tau}_{zi}(a)t(a). \tag{1.28}$$

In the case of open thin walled profiles, however, such a choice for the isolated section portion is suboptimal, unless the $\bar{\tau}_{zi}(a)t(a)$ term is known.

1.4.3 Shear induced stresses in an closed section, thin walled beam

In the case of a closed thin walled, asymmetric section, the search for a point along the wall at which the shear flow may be assumed zero is generally not viable, and the employment of Eq. 1.4.3 in place of the simpler Eq. 1.27 is unavoidable.

In this case, a parametric value for the $\tau_{zs}t$ shear stress flow is assumed for a set of points along the cross section midcurve – one for each elementary closed loop[14] if the points are non-redundantly chosen[15].

In the multicellular cross section example shown in Figure 1.7, two elementary loops are detected; shear flows at the A, B points are parametrically defined as $\tau_A t_A$ and $\tau_B t_B$, respectively.

[13] a linear $d\epsilon_z/dz$ axial strain variation is in fact associated to the curvature variation in z, and not an axial stress variation;

[14] i.e. a closed loop not enclosing any other closed loop.

[15] Redundancy may be pointed out by ideally cutting the cross section at these points: if a monolithic open cross section is obtained, the point choice is not redundant; if a portion of the section is completely isolated, and a loop remains closed, the location of these points causes redundancy.

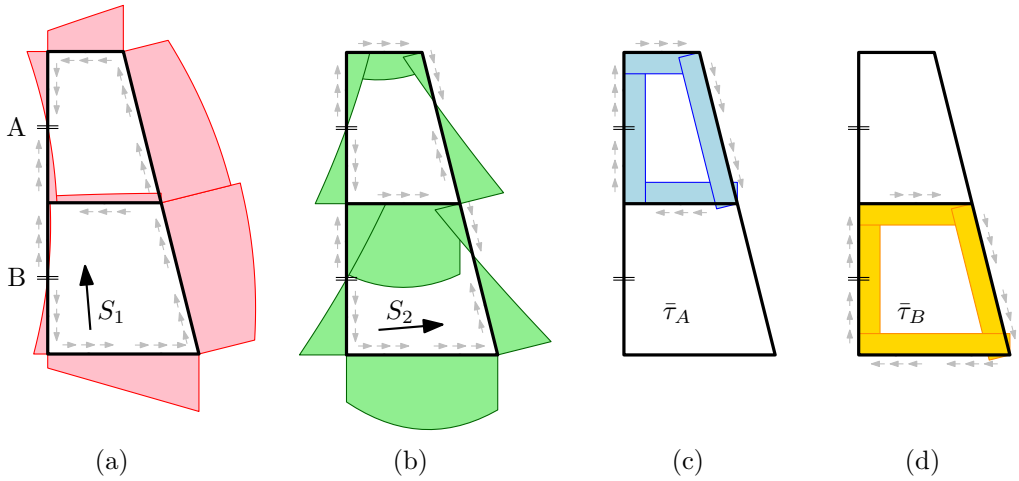

Figure 1.7: XXX.

The τ_{zs} shear stress for each point along the profile wall may then be determined based on Eqn. as a function a) of the shear resultant components S_x and S_y, and b) of the parametrically defined shear stress flows at the A,B points.

Due to the assumed linear response for the profile, superposition principle may be employed in isolating the four elementary contributions to the shear stress flow along the section.

The first two elementary contributions $\tau_{;x}(s)$ and $\tau_{;y}(s)$ are respectively due to the action alone of the x and y shear force components, whose magnitude is assumed equal the product of the stress unit (e.g. 1 MPa) and of the cross sectional area. Those forces are assumed to act in the ideal absence of shear flow at points where the latter is assumed as a parameter (points A and B in Figure 1.7).

Since the condition of zero shear flow is stress-compatible with an opening in the closed section loop, the cross section may be idealized as severed at the assumed shear flow points, and hence open. The equilibrium-based solution procedure derived for the open thin-walled section may hence be profitably applied.

A family of further elementary contributions, one for each of the assumed shear flow points, may be derived by imposing zero parametric shear flow at all the points but the one under scrutiny, and in the

absence of externally applied shear resultants. The elastic problem may be rationalized as an open – initially closed, then ideally severed – thin walled profile, that is loaded by an internal constraint action whose magnitude is unity in terms of stresses. Equilibrium considerations reduce to the conservation of the shear flow due to the absence of $d\sigma_z/dz$ differential axial stress, as in the case of a closed profile under torsion discussed below.

Figures 1.7 (a) and (b) show the shear stress contributions $\tau_{;1}(s)$ and $\tau_{;2}(s)$ induced in the ideally opened (i.e. zero redundant shear flows at the A,B points) multicellar profile by the first and the second shear force components, respectively; due to the author distraction, such figure refers to shear components aligned with the principal directions of bending stiffness, and not to the usual x,y axes.

Figures 1.7 (c) and (d) show the shear stress contributions $\tau_{;A}(s)$ and $\tau_{;B}(s)$ associated to unity values for the parametric shear flows at the A, B segmentation points, respectively.

The cumulative shear stress distribution for the section in Figure 1.7 is

$$\tau(s) = S_1\tau_{;1}(s) + S_2\tau_{;2}(s) + \bar{\tau}_A\tau_{;A}(s) + \bar{\tau}_B\tau_{;B}(s) \tag{1.29}$$

where s is a suitable arclength coordinate.

The associated elastic potential energy may then be integrated over a Δz beam axial portion, thus obtaining

$$\Delta U = \int_s \frac{\tau^2}{G_{sz}} t\Delta z ds \tag{1.30}$$

According to the Castigliano second theorem, the ΔU derivative with respect to the $\bar{\tau}_i$ assumed shear stress value at the i-th segmentation point equates the generalized displacement with respect to which the internal constraint reaction works, i.e. the $t\Delta z\bar{\delta}_i$ integral of the relative longitudinal displacement between the cut surfaces; we hence have

$$\frac{\partial \Delta U}{\partial \bar{\tau}_i} = \bar{\delta}_i t\Delta z \tag{1.31}$$

The $\bar{\delta}_i$ symbol refers to the average value along the $t\Delta z$ area of such axial relative displacement.

Material continùity requires zero $\bar{\delta}_i$ value at each segmentation point, thus defining a set of equations, one for each $\bar{\tau}_i$ unknown parameter, whose solution leads to the definition of the actual shear stress distribution along the closed wall profile.

1.5 Shear stresses due to the St. Venant torsion

The classical solution for the rectilinear beam subject to uniform torsion predicts a displacement field that is composed by the superposition of a) a rigid, in-plane[16] cross section rotation about the shear centre, named twist, of uniform axial rate, and b) an out-of-plane *warping* displacement that is uniform in the axial direction, whereas it varies within the section; such warping displacement is zero in the case of axisymmetric sections only (e.g. solid and hollow circular cross sections).

The in-plane stress components σ_x, σ_y, τ_{xy} are assumed zero, along with the normal stress σ_z. The motion is internally restricted only due to the nonzero out-of-plane shear stresses τ_{yz} and τ_{zx}, that develop as an elastic reaction to the associated strain components.

A more in-depth treatise of the topic involves the solution of an plane, inhomogeneous Laplace differential equation with essential conditions imposed at the cross section boundary, which is beyond the scope of the present contribution.

However, in the case of open- and closed- section, thin walled beams, simplified solutions are available based on the assumptions that a) the out-of-plane shear stresses are locally aligned to the wall midsurface - i.e. $\tau_{zr} = 0$ leaving τ_{zs} as the only nonzero stress component[17], and b) the residual τ_{zs} shear component is either constant by moving through the wall thickness (closed section case), or it linearly varies with the through-thickness coordinate r.

1.5.1 Solid section beam

TODO.

1.5.2 Closed section, thin walled beam

The τ_{sz} component is assumed uniform along the wall thickness, or, equivalently, its deviation from the average value is neglected in calculations.

[16] the rotation vector is actually normal to the cross sectional plane; the *in-plane* motion characterization refers to the associated displacement field.

[17] Here, the notation introduced in paragraph XXX for the thin walled section is employed.

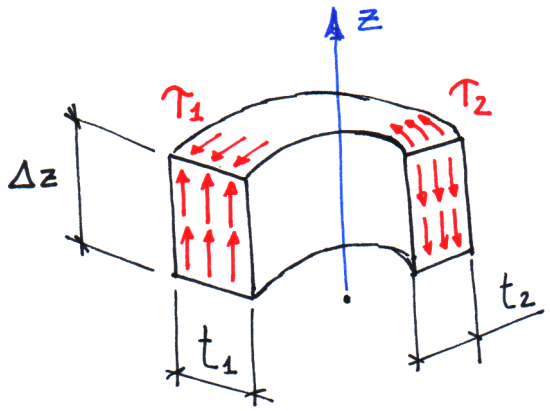

Figure 1.8: Axial equilibrium for a portion of profile wall, in the case of a closed, thin-walled profile subject to torsion.

In the case the material is non-uniform across the thickness, the γ_{sz} shear strain is assumed uniform, whereas the τ_{sz} varies with the varying G_{sz} shear modulus.

In the absence of σ_z, the axial equilibrium of a portion of beam segment dictates that the shear flow $t\tau$ remains constant along the wall, i.e.

$$t_1\tau_1 = t_2\tau_2$$

as depicted in Figure 1.8.

By skipping some further interesting observations (TODO) we may just introduce the Bredt formula for the cross-section torsional stiffness

$$K_t = \frac{4A^2}{\oint \frac{1}{t} dl} \tag{1.32}$$

which is valid for single-celled, closed thin wall sections.

The peak stress is located at thinnest point along the wall, and equals

$$\tau_{\max} = \frac{M_t}{2t_{\min}A} \tag{1.33}$$

.

Multi-celled beam profile? TODO.

1.5.3 Open section, thin walled beam

The shear strain component γ_{zs} is assumed linearly varying across the thickness; if the G_{sz} shear modulus is assumed uniform, such linear variation characterizes the τ_{zs} stress components too.

The average value along the thickness of the τ_{zs} stress component is zero, as zero is the shear flow as defined in the previous paragraph.

For thin enough open sections of uniform and isotropic material we have

$$K_T \approx \frac{1}{3}\int_0^l t^3(s)ds \tag{1.34}$$

If the thin-walled cross section may be described as a sequence of constant thickness wall segments, the simplified formula

$$K_T \approx \frac{1}{3}\sum_i l_i t_i^3 \tag{1.35}$$

is obtained where t_i and l_i are respectively the length and the thickness of each segment.

The peak value for the τ_{zs} stress component is observed in correspondence to thickest wall section point and it equates

$$\tau_{\max} = \frac{M_t t_{\max}}{K_T} \tag{1.36}$$

By applying the reported formulas to a rectangular section whose span length is ten times the wall thickness, the torsional stiffness is overestimated by slightly less than 7%; a similar relative error is reported in terms of shear stress underestimation.

1.6 Castigliano's second theorem and its applications

Castigliano's second theorem may be employed for calculating deflections and rotations, and it states:

> If the strain energy of an elastic structure can be expressed as a function of generalised loads Q_i (namely, forces or moments) then the partial derivative of the strain energy with respect to generalised forces supplies the generalised displacement q_i (namely displacements and rotations with respect to which the generalized forces work).

In equation form,

$$q_i = \frac{\partial U}{\partial Q_i}$$

where U is the strain energy.

1.7 Internal energy for the spatial straight beam

The linear density of the elastic potential (alternatively named internal) energy for the spatial rectilinear beam may be derived as a function of its cross section resultants, namely

$$\frac{dU}{dl} = \frac{J_{\eta\eta}M_\xi^2 + J_{\xi\xi}M_\eta^2 + 2J_{\xi\eta}M_\xi M_\eta}{2E\left(J_{\xi\xi}J_{\eta\eta} - J_{\xi\eta}^2\right)} + \frac{N^2}{2EA} \tag{1.37}$$

$$+ \frac{\chi_\xi S_\xi^2 + \chi_\eta S_\eta^2 + \chi_{\xi\eta}S_\eta S_\xi}{2GA} + \frac{M_t^2}{2GK_t} \tag{1.38}$$

where

- A, $J_{\eta\eta}$, $J_{\xi\xi}$ and $J_{\xi\eta}$ are the section area and moments of inertia, respectively;
- K_t is the section torsional stiffness (**not** generally equivalent to its polar moment of inertia);

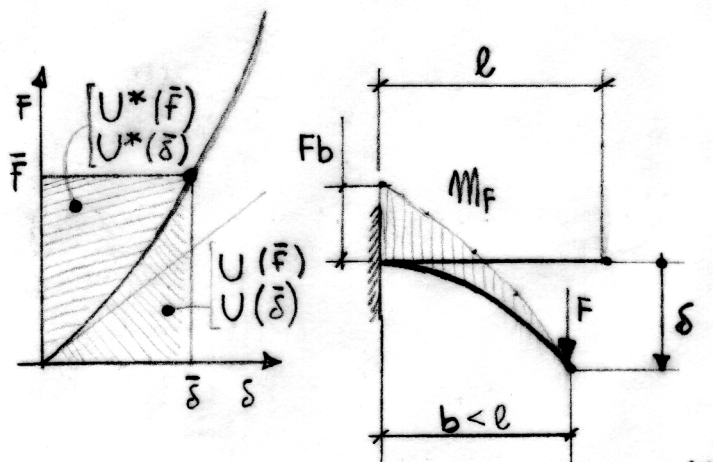

Figure 1.9: A nonlinearly elastic (namely stiffening) structure; the bending moment diagram is evaluated based on the beam portion equilibrium in its *deformed* configuration. The complementary elastic strain energy U^* is plotted for a given applied load $\bar{f}$ or assumed displacement $\bar{\delta}$, alongside the elastic strain energy U.

- E and G are the material Young Modulus and Shear Modulus, respectively; the material is assumed homogeneous, isotropic and linearly elastic.

The shear energy normalized coefficients χ_η,χ_ξ,$\chi_{\xi\eta}$ are specific to the cross section geometry, and may be collected from the expression of the actual shear strain energy due to concurrent action of the S_η, S_ξ shear forces.

In cases of elastically nonlinear structures, the second Castigliano theorem may still be employed, provided that the complementary elastic strain energy U^* is employed in place of the strain energy U, see Fig. 1.9. The two energy terms are equal for linearly behaving structures.

Chapter 2

Fundamentals of Finite Element Method for structural applications

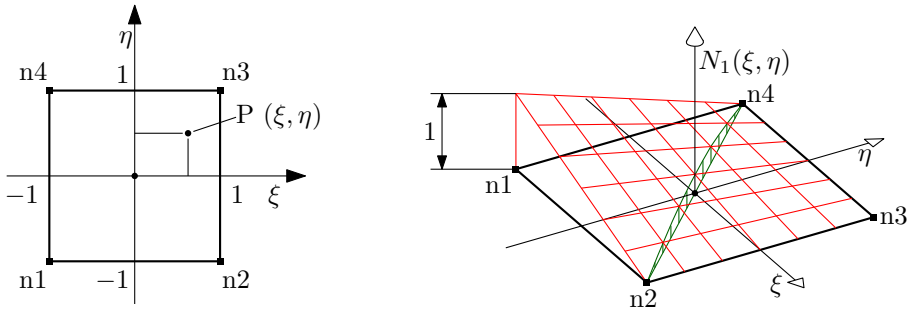

(a) (b)

Figure 2.1: Quadrilateral elementary domain (a), and a representative weight function (b).

2.1 Preliminary results

2.1.1 Interpolation functions for the quadrilateral domain

The elementary quadrilateral domain. A quadrilateral domain is considered whose vertices are conventionally located at the $(\pm 1, \pm 1)$ points of an adimensional (ξ, η) plane coordinate system, see Figure 2.1. Scalar values f_i are associated to a set of *nodal* points $\mathrm{P}_i \equiv [\xi_i, \eta_i]$, which for the present case coincide with the quadrangle vertices, numbered as in Figure.

A $f(\xi, \eta)$ interpolation function may be devised by defining a set of nodal influence functions $N_i(\xi, \eta)$ to be employed as the coefficients (weights) of a moving weighted average

$$f(\xi, \eta) \stackrel{\text{def}}{=} \sum_i N_i(\xi, \eta) f_i \tag{2.1}$$

Requisites for such weight functions are:

- the influence of a node is unitary at its location, whereas the influence of the others locally vanishes, i.e.

  $$N_i(\xi_j, \eta_j) = \delta_{ij} \tag{2.2}$$

  where δ_{ij} is the Kronecker delta function.

- for each point of the domain, the sum of the weights is unitary

$$\sum_i N_i(\xi,\eta) = 1,\ \forall[\xi,\eta] \tag{2.3}$$

Moreover, suitable functions should be continuous and straightforwardly differentiable up to any required degree.

Low order polynomials are ideal candidates for the application; for the particular domain, the nodal weight functions may be stated as

$$N_i(\xi,\eta) \stackrel{\text{def}}{=} \frac{1}{4}\left(1 \pm \xi\right)\left(1 \pm \eta\right), \tag{2.4}$$

where sign ambiguity is resolved for each i-th node by enforcing Eqn. 2.2.

The (2.3) combination of 2.4 functions turns into a general linear relation in (ξ,η) with coplanar in the ξ,η,f space – but otherwise arbitrary – nodal points.

Further generality may be introduced by *not* enforcing coplanarity.

The weight functions for the four-node quadrilateral are in fact quadratic although incomplete[1] in nature, due to the presence of the $\xi\eta$ product, and the absence of any ξ^2,η^2 term.

Each term, and the combined $f(\xi,\eta)$ function, defined as in Eqn. 2.1, behave linearly if restricted to ξ = const. or η = const. loci – namely along the four edges; quadratic behaviour may instead arise along a general direction, e.g. along the diagonals, as in Fig. 2.1b example. Such behaviour is called *bilinear*.

We now consider the $f(\xi,\eta)$ weight function partial derivatives. The partial derivative

$$\frac{\partial f}{\partial \xi} = \underbrace{\left(\frac{f_2 - f_1}{2}\right)}_{[\Delta f/\Delta\xi]_{12}} \underbrace{\left(\frac{1-\eta}{2}\right)}_{N_1+N_2} + \underbrace{\left(\frac{f_3 - f_4}{2}\right)}_{[\Delta f/\Delta\xi]_{43}} \underbrace{\left(\frac{1+\eta}{2}\right)}_{N_4+N_3} = a\eta + b \tag{2.5}$$

linearly varies from the incremental ratio value measured at the $\eta = -1$ lower edge, to the value measured at the $\eta = 1$ upper edge; the other partial derivative

$$\frac{\partial f}{\partial \eta} = \left(\frac{f_4 - f_1}{2}\right)\left(\frac{1-\xi}{2}\right) + \left(\frac{f_3 - f_2}{2}\right)\left(\frac{1+\xi}{2}\right) = c\xi + d. \tag{2.6}$$

[1] or, equivalently, *enriched linear*, as discussed above and in the following

behaves similarly, with $c = a$. However, partial derivatives in ξ, η remain constant along the corresponding differentiation direction [2].

The general quadrilateral domain. The interpolation functions introduced above for the natural quadrilateral may be profitably employed in defining a coordinate mapping between a general quadrangular domain – see Fig. 2.2a – and its reference counterpart, see Figures 2.1 and 2.2b.

In particular, we first define the $\underline{\xi}_i \mapsto \underline{x}_i$ coordinate mapping for the four vertices[3] alone, where ξ, η are the reference (or natural, or elementary) coordinates and x, y are their physical counterpart.

Then, a mapping for the inner points may be derived by interpolation, namely

$$\underline{x} = \underline{m}\left(\underline{\xi}\right) = \sum_{i=1}^{4} N_i\left(\underline{\xi}\right) \underline{x}_i \tag{2.7}$$

The availability of an inverse $\underline{m}^{-1} : \underline{x} \mapsto \underline{\xi}$ mapping is not granted; in particular, a closed form representation for such inverse is not generally available[4].

In the absence of an handy inverse mapping function, it is convenient to reinstate the interpolation procedure obtained for the natural domain, i.e.

$$f(\xi, \eta) \stackrel{\text{def}}{=} \sum_i N_i(\xi, \eta) f_i \tag{2.8}$$

The four f_i nodal values are interpolated based on the *natural* ξ, η coordinates of an inner P point, and not as a function of its physical x, y coordinates, that are never promoted to the independent variable role.

As already mentioned, the $\underline{m}$ mapping behaves linearly along η =const. and ξ =const. one dimensional subdomains, and in particular along the quadrangle edges[5]; the inverse mapping $\underline{m}^{-1}$ exists along these line

[2] The relevance of such partial derivative orders will appear clearer to the reader once the strain field will have been derived in paragraph XXX.

[3] The condensed notation $\underline{\xi}_i \equiv (\xi_i, \eta_i)$, $\underline{x}_i \equiv (x_i, y_i)$ for coordinate vectors is employed.

[4] For a given $\bar{\underline{x}}$ physical point, however, Newton-Raphson iterations rapidly converge to the $\bar{\underline{\xi}} = \underline{m}^{-1}(\bar{\underline{x}})$ solution if the centroid is chosen for algorithm initialization, see Section XXX

[5] see paragraph XXX

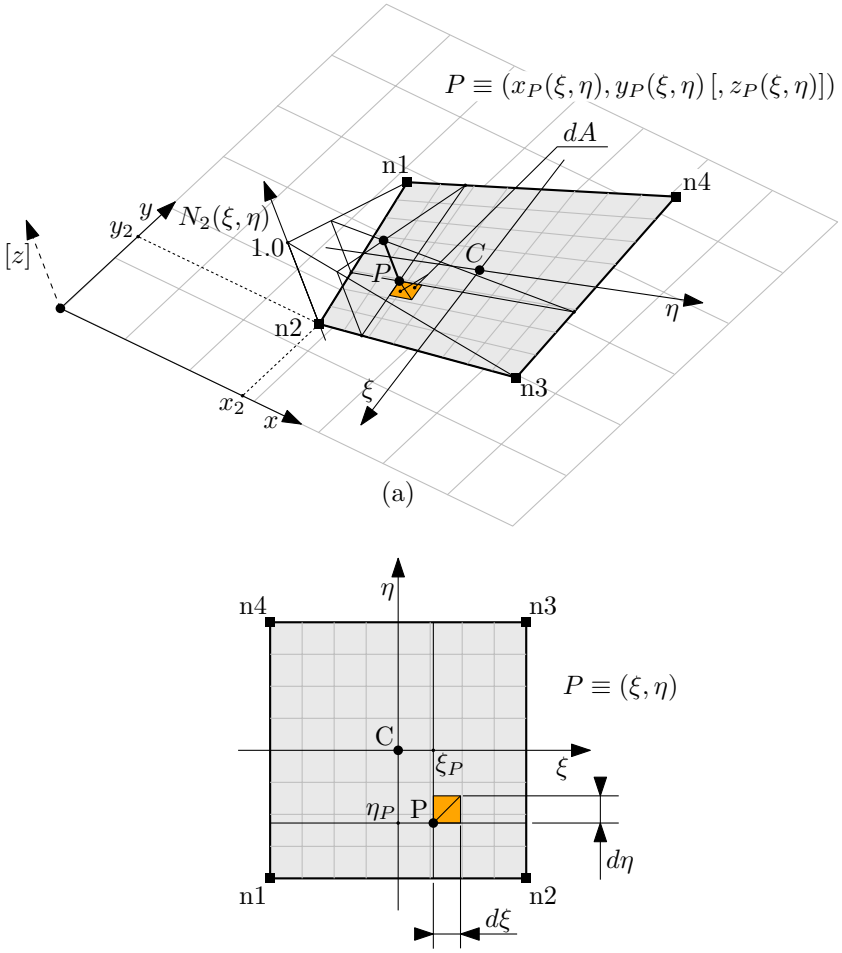

Figure 2.2: Quadrilateral general domain, (a), and its reference counterpart (b). If the general quadrangle is defined within a spatial environment, and not as a figure lying on the xy plane, limited z_i offsets are allowed at nodes with respect to such plane, which are not considered in Figure.

segments under the further condition that their length is nonzero[6], and it is a linear function[7] . Being a composition of linear functions, the interpolation function $f(\underline{\mathrm{m}}^{-1}(x,y))$ is also linear along the aforementioned subdomains, and in particular along the quadrangle edges.

The directional derivatives of f with respect to x or y are obtained based the indirect relation

$$\begin{bmatrix} \frac{\partial f}{\partial \xi} \\ \frac{\partial f}{\partial \eta} \end{bmatrix} = \underbrace{\begin{bmatrix} \frac{\partial x}{\partial \xi} & \frac{\partial y}{\partial \xi} \\ \frac{\partial x}{\partial \eta} & \frac{\partial y}{\partial \eta} \end{bmatrix}}_{\underline{\underline{\mathrm{J}}}'(\xi,\eta)} \begin{bmatrix} \frac{\partial f}{\partial x} \\ \frac{\partial f}{\partial y} \end{bmatrix} \tag{2.9}$$

.

The function derivatives with respect to ξ, η are obtained as

$$\begin{bmatrix} \frac{\partial f}{\partial \xi} \\ \frac{\partial f}{\partial \eta} \end{bmatrix} = \sum_i \begin{bmatrix} \frac{\partial N_i}{\partial \xi} \\ \frac{\partial N_i}{\partial \eta} \end{bmatrix} f_i. \tag{2.10}$$

The *transposed* Jacobian matrix of the mapping function that appears in 2.9 is

$$\underline{\underline{\mathrm{J}}}'(\xi,\eta) = \begin{bmatrix} \frac{\partial x}{\partial \xi} & \frac{\partial y}{\partial \xi} \\ \frac{\partial x}{\partial \eta} & \frac{\partial y}{\partial \eta} \end{bmatrix} \tag{2.11}$$

$$= \sum_i \left(\begin{bmatrix} \frac{\partial N_i}{\partial \xi} & 0 \\ \frac{\partial N_i}{\partial \eta} & 0 \end{bmatrix} x_i + \begin{bmatrix} 0 & \frac{\partial N_i}{\partial \xi} \\ 0 & \frac{\partial N_i}{\partial \eta} \end{bmatrix} y_i \right) \tag{2.12}$$

If the latter matrix is assumed nonsingular – condition, this, that pairs the bijective nature of the $\underline{\mathrm{m}}$ mapping, equation 2.9 may be inverted, thus leading to the form

$$\begin{bmatrix} \frac{\partial f}{\partial x} \\ \frac{\partial f}{\partial y} \end{bmatrix} = \left(\underline{\underline{\mathrm{J}}}' \right)^{-1} \begin{bmatrix} \dots & \frac{\partial N_i}{\partial \xi} & \dots \\ \dots & \frac{\partial N_i}{\partial \eta} & \dots \end{bmatrix} \begin{bmatrix} \vdots \\ f_i \\ \vdots \end{bmatrix}, \tag{2.13}$$

[6]The case exists of an edge whose endpoints are superposed, i.e. the edge collapses to a point.

[7]A constructive proof may be defined for each edge by retrieving the non-uniform amongst the ξ, η coordinates, namely λ, as the ratio

$$\lambda = 2\frac{(x_Q - x_i)(x_j - x_i) + (y_Q - y_i)(y_j - y_i)}{(x_j - x_i)^2 + (y_j - y_i)^2} - 1,$$

where Q is a generic point along the edge, and i,j are the two subdomain endpoints at which λ equates -1 and $+1$, respectively. A similar function may be defined for any constant ξ, η segment.

where the inner mechanics of the matrix-vector product are appointed for the Eq. 2.10 summation.

2.1.2 Gaussian quadrature rules for some relevant domains.

Reference one dimensional domain. The gaussian quadrature rule for approximating the definite integral of a $f(\xi)$ function over the $[-1, 1]$ reference interval is constructed as the customary weighted sum of internal function samples, namely

$$\int_{-1}^{1} f(\xi)d\xi \approx \sum_{i=1}^{n} f(\xi_i)w_i; \tag{2.14}$$

Its peculiarity is to employ location-weight pairs (ξ_i, w_i) that are optimal with respect to the polynomial class of functions. Nevertheless, such choice has revealed itself to be robust enough for for a more general employment.

Let's consider a m-th order polynomial

$$p(\xi) \stackrel{\text{def}}{=} a_m\xi^m + a_{m-1}\xi^{m-1} + ... + a_1\xi + a_0$$

whose exact integral is

$$\int_{-1}^{1} p(\xi)d\xi = \sum_{j=0}^{m} \frac{(-1)^j + 1}{j+1} a_j$$

The integration residual between the exact definite integral and the weighted sample sum is defined as

$$r\left(a_j, (\xi_i, w_i)\right) \stackrel{\text{def}}{=} \sum_{i=1}^{n} p(\xi_i)w_i - \int_{-1}^{1} p(\xi)d\xi \tag{2.15}$$

The optimality condition is stated as follows: the quadrature rule involving n sample points (ξ_i, w_i), $i = 1 ... n$ is optimal for the m-th order polynomial if a) the integration residual is null for general a_j values , and b) such condition does not hold for any lower-order sampling rule.

Once observed that the zero residual requirement is satisfied by any sampling rule if the polynomial a_j coefficients are all null, condition

a) may be enforced by imposing that such zero residual value remains constant with varying a_j terms, i.e.

$$\begin{cases} \dfrac{\partial r\left(a_j,(\xi_i,w_i)\right)}{\partial a_j}=0, \quad j=0\,...\,m \end{cases} \tag{2.16}$$

A system of $m+1$ polynomial equations of degree $m-1$ is hence obtained in the $2n$ (ξ_i, w_i) unknowns; in the assumed absence of redundant equations, solutions do not exist if the constraints outnumber the unknowns, i.e. $m > 2n-1$. Limiting our discussion to the threshold condition $m = 2n-1$, an attentive algebraic manipulation of Eqns. 2.16 may be performed in order to extract the (ξ_i, w_i) solutions, which are unique apart from the pair permutations[8].

Eqns. 2.16 solutions are reported in Table 2.1 for quadrature rules with up to $n = 4$ sample points[9].

It is noted that the integration points are symmetrically distributed with respect to the origin, and that the function is never sampled at the $\{-1, 1\}$ extremal points.

[8] In this note, location-weight pairs are obtained for the gaussian quadrature rule of order $n = 2$, aiming at illustrating the general procedure. The general $m = 2n-1 = 3$rd order polynomial is stated in the form

$$p(\xi)=a_3\xi^3+a_2\xi^2+a_1\xi+a_0, \quad \int_{-1}^{1} p(\xi)d\xi=\frac{2}{3}a_2+2a_0,$$

whereas the integral residual is

$$r=a_3\left(w_1\xi_1^3+w_2\xi_2^3\right)+a_2\left(w_1\xi_1^2+w_2\xi_2^2-\frac{2}{3}\right)+a_1\left(w_1\xi_1+w_2\xi_2\right)+a_0\left(w_1+w_2-2\right)$$

Eqns 2.16 may be derived as

$$\begin{cases} 0=\frac{\partial r}{\partial a_3}=w_1\xi_1^3+w_2\xi_2^3 & (e_1)\\ 0=\frac{\partial r}{\partial a_2}=w_1\xi_1^2+w_2\xi_2^2-\frac{2}{3} & (e_2)\\ 0=\frac{\partial r}{\partial a_1}=w_1\xi_1+w_2\xi_2 & (e_3)\\ 0=\frac{\partial r}{\partial a_0}=w_1+w_2-2 & (e_4) \end{cases}$$

which are independent of the a_j coefficients.

By composing $\left(e_1-\xi_1^2 e_3\right)/(w_2\xi_2)$ it is obtained that $\xi_2^2=\xi_1^2$; e_2 may then be written as $(w_1+w_2)\xi_1^2=2/3$, and then as $2\xi_1^2=2/3$, according to e_4. It derives that $\xi_{1,2}=\pm 1/\sqrt{3}$. Due to the opposite nature of the roots, e_3 implies $w_2=w_1$, relation, this, that turns e_4 into $2w_1=2w_2=2$, and hence $w_{1,2}=1$.

[9] see `https://pomax.github.io/bezierinfo/legendre-gauss.html` for higher order gaussian quadrature rule sample points.

n	ξ_i	w_i
1	0	2
2	$\pm\frac{1}{\sqrt{3}}$	1
3	0 $\pm\sqrt{\frac{3}{5}}$	$\frac{8}{9}$ $\frac{5}{9}$
4	$\pm\sqrt{\frac{3}{7}-\frac{2}{7}\sqrt{\frac{6}{5}}}$ $\pm\sqrt{\frac{3}{7}+\frac{2}{7}\sqrt{\frac{6}{5}}}$	$\frac{18+\sqrt{30}}{36}$ $\frac{18-\sqrt{30}}{36}$

Table 2.1: Integration points for the lower order gaussian quadrature rules.

General one dimensional domain. The extension of the one dimensional quadrature rule from the reference domain $[-1,1]$ to a general $[a,b]$ domain is pretty straightforward, requiring just a change of integration variable to obtain the following

$$\begin{aligned}\int_a^b f(x)dx &= \frac{b-a}{2}\int_{-1}^{1} f\left(\frac{b+a}{2}+\frac{b-a}{2}\xi\right)d\xi,\\ &\approx \frac{b-a}{2}\sum_{i=1}^{n} f\left(\frac{b+a}{2}+\frac{b-a}{2}\xi_i\right)w_i.\end{aligned}$$

Reference quadrangular domain. A quadrature rule for the reference quadrangular domain of Figure 2.1a may be derived by nesting the quadrature rule defined for the reference interval, see Eqn. 2.14, thus obtaining

$$\int_{-1}^{1}\int_{-1}^{1} f(\xi,\eta)\,d\xi d\eta \approx \sum_{i=1}^{p}\sum_{j=1}^{q} f\left(\xi_i,\eta_j\right)w_i w_j \tag{2.17}$$

where (ξ_i, w_i) and (η_j, w_j) are the coordinate-weight pairs of the two quadrature rules of p and q order, respectively, employed for spanning the two coordinate axes. The equivalent notation

$$\int_{-1}^{1}\int_{-1}^{1} f(\xi,\eta)\,d\xi d\eta \approx \sum_{l=1}^{pq} f\left(\underline{\xi}_l\right)w_l \tag{2.18}$$

emphasises the characteristic nature of the pq point/weight pairs for the domain and for the quadrature rule employed; a general integer bijection[10] $\{1 \dots pq\} \leftrightarrow \{1 \dots p\} \times \{1 \dots q\}$, $l \leftrightarrow (i, j)$ may be utilized to formally derive the two-dimensional quadrature rule pairs

$$\underline{\xi}_l = \left(\xi_i, \eta_j\right), \quad w_l = w_i w_j, \quad l = 1 \dots pq \tag{2.19}$$

from their uniaxial counterparts.

General quadrangular domain. The rectangular infinitesimal area $dA_{\xi\eta} = d\xi d\eta$ in the neighborhood of a ξ_P, η_P location, see Figure 2.2b, is mapped to the quadrangle of Figure 2.2a, which is composed by the two triangular areas

$$\begin{aligned} dA_{xy} = \quad & \frac{1}{2!}\begin{vmatrix} 1 & x\left(\xi_P \quad\;\; , \eta_P \quad\;\; \right) & y\left(\xi_P \quad\;\; , \eta_P \quad\;\; \right) \\ 1 & x\left(\xi_P + d\xi, \eta_P \quad\;\; \right) & y\left(\xi_P + d\xi, \eta_P \quad\;\; \right) \\ 1 & x\left(\xi_P \quad\;\; , \eta_P + d\eta\right) & y\left(\xi_P \quad\;\; , \eta_P + d\eta\right) \end{vmatrix} + \\ & + \frac{1}{2!}\begin{vmatrix} 1 & x\left(\xi_P + d\xi, \eta_P + d\eta\right) & y\left(\xi_P + d\xi, \eta_P + d\eta\right) \\ 1 & x\left(\xi_P \quad\;\; , \eta_P + d\eta\right) & y\left(\xi_P \quad\;\; , \eta_P + d\eta\right) \\ 1 & x\left(\xi_P + d\xi, \eta_P \quad\;\; \right) & y\left(\xi_P + d\xi, \eta_P \quad\;\; \right) \end{vmatrix}. \end{aligned} \tag{2.20}$$

The determinant formula for the area of a triangle, shown below along with its n-dimensional symplex hypervolume generalization,

$$\mathcal{A} = \frac{1}{2!}\begin{vmatrix} 1 & x_1 & y_1 \\ 1 & x_2 & y_2 \\ 1 & x_3 & y_3 \end{vmatrix}, \quad \mathcal{H} = \frac{1}{n!}\begin{vmatrix} 1 & \underline{\mathrm{x}}_1 \\ 1 & \underline{\mathrm{x}}_2 \\ \vdots & \vdots \\ 1 & \underline{\mathrm{x}}_{n+1} \end{vmatrix} \tag{2.21}$$

has been employed above.

[10] e.g.

$$\{i-1; j-1\} = (l-1) \bmod (p, q), \quad l - 1 = (j-1)q + (i-1)$$

where the operator

$$\{a_n; \dots; a_3; a_2; a_1\} = m \bmod (b_n, \dots, b_3, b_2, b_1)$$

consists in the extraction of the n least significant a_i digits of a mixed radix representation of the integer m with respect to the sequence of b_i bases, with $i = 1 \dots n$.

By operating a local multivariate linearization of the 2.20 matrix terms, the relation

$$dA_{xy} \approx \frac{1}{2!}\begin{vmatrix} 1 & x & y \\ 1 & x + x_{,\xi}d\xi & y + y_{,\xi}d\xi \\ 1 & x + x_{,\eta}d\eta & y + y_{,\eta}d\eta \end{vmatrix} + \\ + \frac{1}{2!}\begin{vmatrix} 1 & x + x_{,\xi}d\xi + x_{,\eta}d\eta & y + y_{,\xi}d\xi + y_{,\eta}d\eta \\ 1 & x + x_{,\eta}d\eta & y + y_{,\eta}d\eta \\ 1 & x + x_{,\xi}d\xi & y + y_{,\xi}d\xi \end{vmatrix}$$

is obtained, where $x, y, x_{,\xi}, x_{,\eta}, y_{,\xi}$, and $y_{,\eta}$ are the x, y functions and their first order partial derivatives, sampled at the (ξ_P, η_P) point; infinitesimal terms of order higher than $d\xi, d\eta$ are neglected.

After some matrix manipulations[11], the following expression is obtained

$$dA_{xy} = \begin{vmatrix} 1 & 0 & 0 \\ 0 & x_{,\xi} & y_{,\xi} \\ 0 & x_{,\eta} & y_{,\eta} \end{vmatrix} d\xi d\eta = \underbrace{\begin{vmatrix} x_{,\xi} & y_{,\xi} \\ x_{,\eta} & y_{,\eta} \end{vmatrix}}_{|J^{\mathrm{T}}(\xi_P, \eta_P)|} dA_{\xi\eta} \tag{2.22}$$

that equates the ratio of the mapped and of the reference areas to the determinant of the transformation (transpose) Jacobian matrix[12].

After the preparatory passages above, we obtain

$$\iint_{A_{xy}} g(x, y) dA_{xy} = \iint_{-1}^{1} g\left(x\left(\xi, \eta\right), y\left(\xi, \eta\right)\right) \left|J(\xi, \eta)\right| d\xi d\eta, \tag{2.23}$$

thus reducing the quadrature over a general domain to its reference domain counterpart, which has been discussed in the paragraph above.

[11] For both the determinants, the first column is multiplied by x_P and subtracted to the second column, and then subtracted to the third column once multiplied by y_P. The first row is then subtracted to the others. On the second determinant alone, both the second and the third columns are changed in sign; then, the second and the third rows are summed to the first. The two determinants are now formally equal, and the two 1/2 multipliers are summed to provide unity. The $d\xi$ and the $d\eta$ factors may then be collected from the second and the third rows, respectively.

[12] The Jacobian matrix for a general $\underline{\xi} \mapsto \underline{x}$ mapping is in fact defined according to

$$[J(\underline{\xi}_P)]_{ij} \stackrel{\text{def}}{=} \left.\frac{\partial x_i}{\partial \xi_j}\right|_{\underline{\xi} = \underline{\xi}_P} \qquad i, j = 1 \dots n$$

being i the generic matrix term row index, and j the column index

Based on Eqn. 2.18, the quadrature rule

$$\iint_{A_{xy}} g(\underline{\mathrm{x}})dA_{xy} \approx \sum_{l=1}^{pq} g\left(\underline{\mathrm{x}}\left(\underline{\xi}_l\right)\right)\left|J(\underline{\xi}_l)\right| w_l \tag{2.24}$$

is derived, stating that the definite integral of a g integrand over a quadrangular domain pertaining to the physical x, y plane (x, y are dimensional quantities, namely lengths) may be approximated as follows:

1. a reference-to-physical domain mapping is defined, that is based on the vertex physical coordinate interpolation;

2. the function is sampled at the physical locations that are the images of the Gaussian integration points previously obtained for the reference domain;

3. a weighted sum of the collected samples is performed, where the weights consist in the product of i) the adimensional w_l Gauss point weight (suitable for integrating on the reference domain), and ii) a dimensional area scaling term, that equals the determinant of the transformation Jacobian matrix, locally evaluated at the Gauss points.

2.2 Basic theory of plates

P displacement components as a function of the Q reference point motion.

$$u_P = u + z\,(1 + \tilde{\epsilon}_z)\,sin\,\phi \tag{2.25}$$
$$v_P = v - z\,(1 + \tilde{\epsilon}_z)\,sin\,\theta \tag{2.26}$$
$$w_P = w + z\,((1 + \tilde{\epsilon}_z)\,cos(\phi)\,cos(\theta) - 1) \tag{2.27}$$

$$\tilde{\epsilon}(z) = \frac{1}{z}\int_0^z \epsilon_z d\varsigma \tag{2.28}$$
$$= \frac{1}{z}\int_0^z \left(-\nu\epsilon_x - \nu\epsilon_y\right) d\varsigma \tag{2.29}$$

P displacement components as a function of the Q reference point motion, linarized with respect to the small rotations and small strain hypotheses.

$$u_P = u + z\phi \tag{2.30}$$
$$v_P = v - z\theta \tag{2.31}$$
$$w_P = w \tag{2.32}$$

Relation between the normal displacement x, y gradient (i.e. the deformed plate slope), the rotations and the out-of-plane, interlaminar, averaged shear strain components.

$$\frac{\partial w}{\partial x} = \bar{\gamma}_{zx} - \phi \tag{2.33}$$
$$\frac{\partial w}{\partial y} = \bar{\gamma}_{yz} + \theta \tag{2.34}$$

Strains at point P.

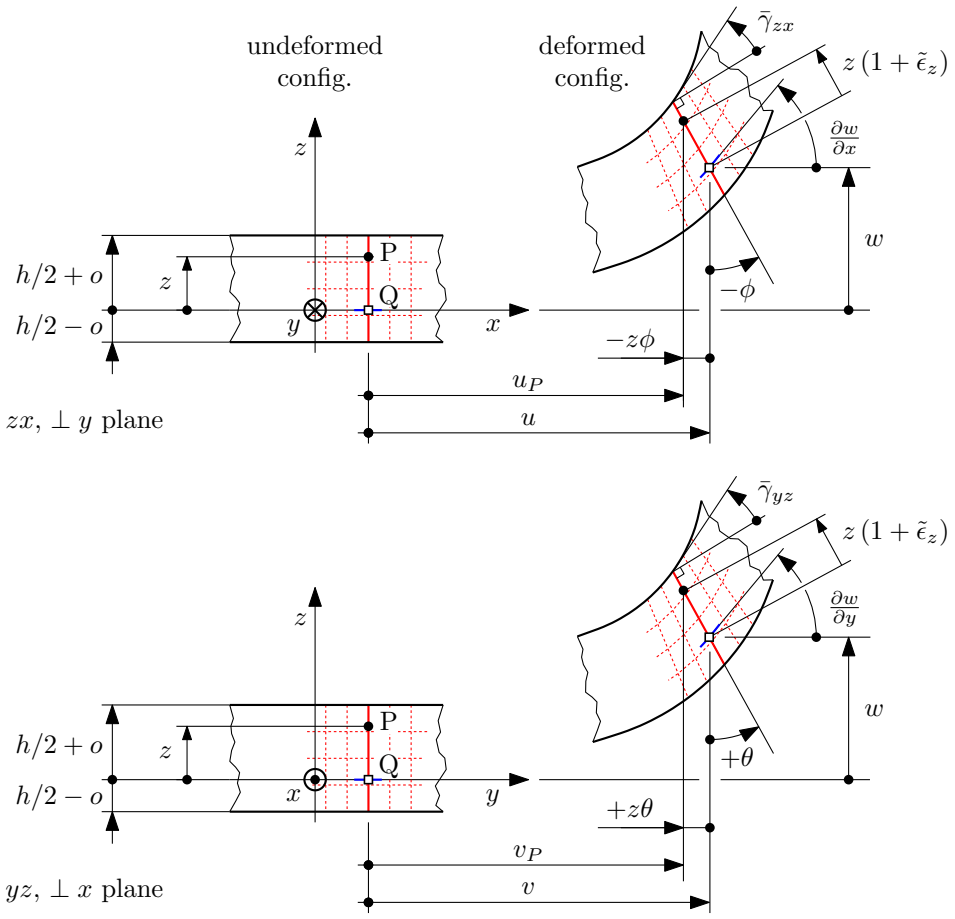

Figure 2.3: Relevant dimensions for describing the deformable plate kinematics.

$$\epsilon_x = \frac{\partial u_P}{\partial x} = \frac{\partial u}{\partial x} + z\frac{\partial \phi}{\partial x} \tag{2.35}$$

$$\epsilon_y = \frac{\partial v_P}{\partial y} = \frac{\partial v}{\partial y} - z\frac{\partial \theta}{\partial y} \tag{2.36}$$

$$\gamma_{xy} = \frac{\partial u_P}{\partial y} + \frac{\partial v_P}{\partial x} \tag{2.37}$$

$$= \left(\frac{\partial u}{\partial y} + \frac{\partial v}{\partial x}\right) + z\left(+\frac{\partial \phi}{\partial y} - \frac{\partial \theta}{\partial x}\right) \tag{2.38}$$

Generalized plate strains: membrane strains.

$$\underline{\bar{\epsilon}} = \begin{pmatrix} \frac{\partial u}{\partial x} \\ \frac{\partial v}{\partial y} \\ \frac{\partial u}{\partial y} + \frac{\partial v}{\partial x} \end{pmatrix} = \begin{pmatrix} \bar{\epsilon}_x \\ \bar{\epsilon}_y \\ \bar{\gamma}_{xy} \end{pmatrix} \tag{2.39}$$

Generalized plate strains: curvatures.

$$\underline{\kappa} = \begin{pmatrix} +\frac{\partial \phi}{\partial x} \\ -\frac{\partial \theta}{\partial y} \\ +\frac{\partial \phi}{\partial y} - \frac{\partial \theta}{\partial x} \end{pmatrix} = \begin{pmatrix} \kappa_x \\ \kappa_y \\ \kappa_{xy} \end{pmatrix} \tag{2.40}$$

Compact form for the strain components at P.

$$\underline{\epsilon} = \underline{\bar{\epsilon}} + z\,\underline{\kappa} \tag{2.41}$$

Hook law for an isotropic material, under plane stress conditions.

$$\underline{\underline{D}} = \frac{E}{1-\nu^2}\begin{pmatrix} 1 & \nu & 0 \\ \nu & 1 & 0 \\ 0 & 0 & \frac{1-\nu}{2} \end{pmatrix} \tag{2.42}$$

Normal components for stress and strain, the latter for the isotropic material case only.

$$\sigma_z = 0 \tag{2.43}$$

$$\epsilon_z = -\nu\left(\epsilon_x + \epsilon_y\right) \tag{2.44}$$

Stresses at P.

$$\underline{\sigma} = \underline{\underline{D}}\,\underline{\epsilon} = \underline{\underline{D}}\,\underline{\bar{\epsilon}} + z\,\underline{\underline{D}}\,\underline{\kappa} \tag{2.45}$$

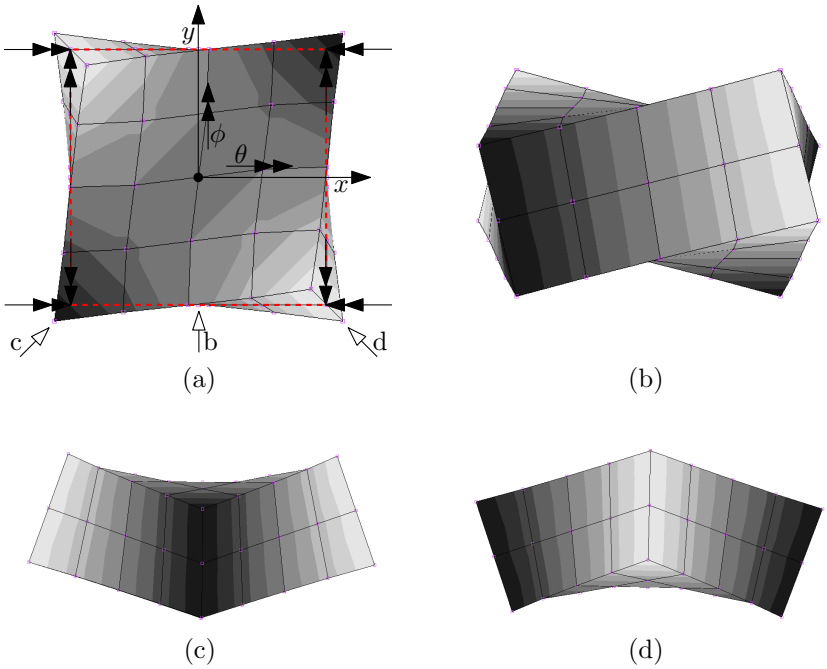

Figure 2.4: Positive κ_{xy} torsional curvature for the plate element. Subfigure (a) shows the positive γ_{xy} shear strain at the upper surface, the (in-plane) undeformed midsurface, and the negative γ_{xy} at the lower surface; the point of sight related to subfigures (b) to (d) are also evidenced. θ and ϕ rotation components decrease with x and increase with y, respectively, thus leading to positive κ_{xy} contributions. As shown in subfigures (c) and (d), the torsional curvature of subfigure (b) evolves into two anticlastic bending curvatures if the reference system is aligned with the square plate element diagonals, and hence rotated by 45° with respect to z.

Membrane (direct and shear) stress resultants (shear flows).

$$\underline{\mathrm{q}} = \begin{pmatrix} q_x \\ q_y \\ q_{xy} \end{pmatrix} = \int_h \underline{\sigma}\, dz \tag{2.46}$$

$$= \underbrace{\int_h \underline{\underline{\mathrm{D}}}\, dz}_{\underline{\underline{\mathrm{A}}}}\, \underline{\bar{\epsilon}} + \underbrace{\int_h \underline{\underline{\mathrm{D}}}\, z dz}_{\underline{\underline{\mathrm{B}}}}\, \underline{\kappa} \tag{2.47}$$

Bending and torsional moment stress resultants (moment flows).

$$\underline{\mathrm{m}} = \begin{pmatrix} m_x \\ m_y \\ m_{xy} \end{pmatrix} = \int_h \underline{\sigma}\, dz \tag{2.48}$$

$$= \underbrace{\int_h \underline{\underline{\mathrm{D}}}\, z dz}_{\underline{\underline{\mathrm{B}}} \equiv \underline{\underline{\mathrm{B}}}^{\mathrm{T}}}\, \underline{\bar{\epsilon}} + \underbrace{\int_h \underline{\underline{\mathrm{D}}}\, z^2 dz}_{\underline{\underline{\mathrm{C}}}}\, \underline{\kappa} \tag{2.49}$$

Cumulative generalized strain - stress relations for the plate (or for the laminate)

$$\begin{pmatrix} \underline{\mathrm{q}} \\ \underline{\mathrm{m}} \end{pmatrix} = \begin{pmatrix} \underline{\underline{\mathrm{A}}} & \underline{\underline{\mathrm{B}}} \\ \underline{\underline{\mathrm{B}}}^{\mathrm{T}} & \underline{\underline{\mathrm{C}}} \end{pmatrix} \begin{pmatrix} \underline{\bar{\epsilon}} \\ \underline{\kappa} \end{pmatrix} \tag{2.50}$$

Hook law for the orthotropic material in plane stress conditions, with respect to principal axes of orthotropy;

$$\underline{\underline{\mathrm{D}}}_{123} = \begin{pmatrix} \frac{E_1}{1-\nu_{12}\nu_{21}} & \frac{\nu_{21}E_1}{1-\nu_{12}\nu_{21}} & 0 \\ \frac{\nu_{12}E_2}{1-\nu_{12}\nu_{21}} & \frac{E_2}{1-\nu_{12}\nu_{21}} & 0 \\ 0 & 0 & G_{12} \end{pmatrix} \tag{2.51}$$

$$\begin{pmatrix} \sigma_1 \\ \sigma_2 \\ \tau_{12} \end{pmatrix} = \underline{\underline{\mathrm{T}}}_1 \begin{pmatrix} \sigma_x \\ \sigma_y \\ \tau_{xy} \end{pmatrix} \qquad \begin{pmatrix} \epsilon_1 \\ \epsilon_2 \\ \gamma_{12} \end{pmatrix} = \underline{\underline{\mathrm{T}}}_2 \begin{pmatrix} \epsilon_x \\ \epsilon_y \\ \gamma_{xy} \end{pmatrix} \tag{2.52}$$

where

$$\underline{\underline{\mathrm{T}}}_1 = \begin{pmatrix} m^2 & n^2 & 2mn \\ n^2 & m^2 & -2mn \\ -mn & mn & m^2 - n^2 \end{pmatrix} \tag{2.53}$$

$$\underline{\underline{\mathrm{T}}}_2 = \begin{pmatrix} m^2 & n^2 & mn \\ n^2 & m^2 & -mn \\ -2mn & 2mn & m^2 - n^2 \end{pmatrix} \tag{2.54}$$

α is the angle between 1 and x;

$$m = cos(\alpha) \qquad\qquad n = sin(\alpha) \tag{2.55}$$

The inverse transformations may be obtained based on the relations

$$\underline{\underline{\mathrm{T}}}_1^{-1}(+\alpha) = \underline{\underline{\mathrm{T}}}_1(-\alpha) \qquad \underline{\underline{\mathrm{T}}}_2^{-1}(+\alpha) = \underline{\underline{\mathrm{T}}}_2(-\alpha) \tag{2.56}$$

Finally

$$\underline{\sigma} = \underline{\underline{\mathrm{D}}}\,\underline{\epsilon} \qquad \underline{\underline{\mathrm{D}}} \equiv \underline{\underline{\mathrm{D}}}_{xyz} = \underline{\underline{\mathrm{T}}}_1^{-1}\,\underline{\underline{\mathrm{D}}}_{123}\,\underline{\underline{\mathrm{T}}}_2 \tag{2.57}$$

Notes:

- Midplane is ill-defined if the material distribution is not symmetric; the geometric midplane (i.e. the one obtained by ignoring the material distribution) exhibits no relevant properties in general. Its definition is nevertheless pretty straighforward.
- If the unsimmetric laminate is composed by isotropic layers, a reference plane may be obtained for which the $\underline{\underline{\mathrm{B}}}$ membrane-to-bending coupling matrix vanishes; a similar condition may not be verified in the presence of orthotropic layers.
- Thermally induced distortion is not self-compensated in an unsymmetric laminate even if the temperature is held constant through the thickness.

2.3 The bilinear isoparametric shear-deformable shell element

Once gathered the required algebraic paraphernalia, the definition of a bilinear quadrilateral shear-deformable isoparametric shell element is straightforward.

The quadrilateral element geometry is defined by the position in space of its four vertices, named *nodes*; a global reference system $OXYZ$ is employed for dealing with multiple elements (i.e. at a whole model scale), whereas a more convenient, local $oxyz$ reference system is used when a single element is under scrutiny – e.g. in the current paragraph.

A function that interpolates along the quadrilateral domain the values a given quantity assumes at nodes has been introduced in paragraph 2.1.1; such function depends on the normalized coordinate pair $\xi, \eta \in [-1, 1]$ that spans the elementary quadrilateral of Figure 2.1.

The element degrees of freedom consist in the displacements and the rotations of the four quadrilateral vertices, named *nodes*.

> This is a four-node, thick-shell element with global displacements and rotations as degrees of freedom. Bilinear interpolation is used for the coordinates, displacements and the rotations. The membrane strains are obtained from the displacement field; the curvatures from the rotation field. The transverse shear strains are calculated at the middle of the edges and interpolated to the integration points. In this way, a very efficient and simple element is obtained which exhibits correct behavior in the limiting case of thin shells. The element can be used in curved shell analysis as well as in the analysis of complicated plate structures. For the latter case, the element is easy to use since connections between intersecting plates can be modeled without tying. Due to its simple formulation when compared to the standard higher order shell elements, it is less expensive and, therefore, very attractive in nonlinear analysis. The element is not very sensitive to distortion, particularly if the corner nodes lie in the same plane. All constitutive relations can be used with this element.

Chapter 3

Miscellaneous

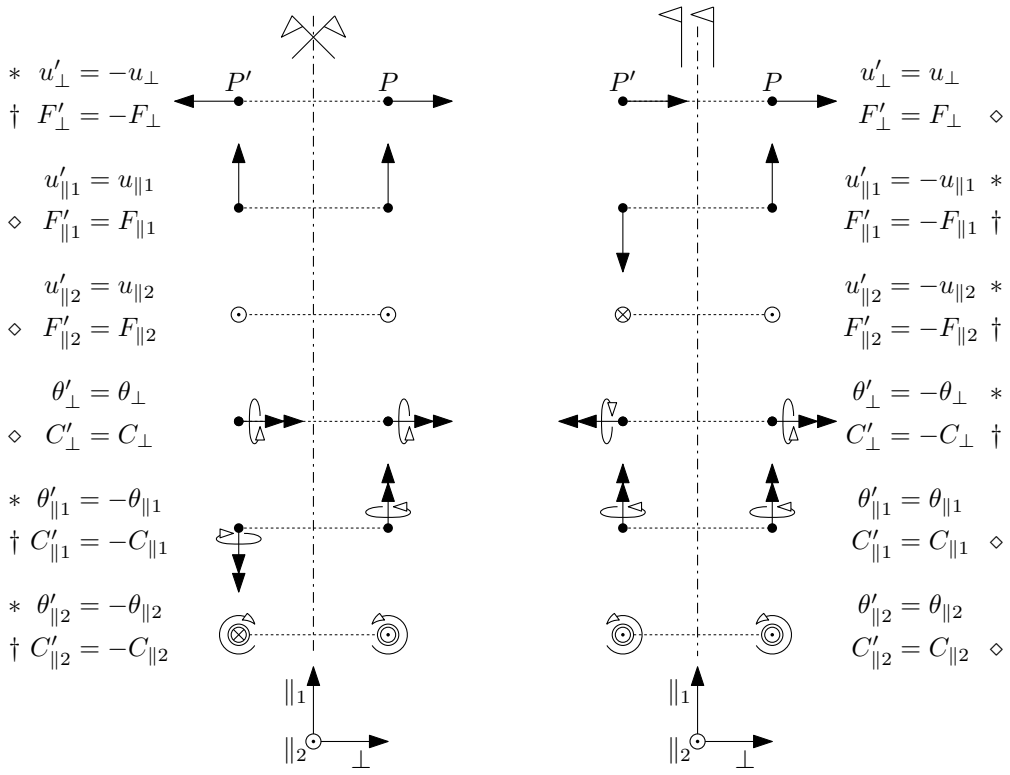

Figure 3.1: An overview of symmetrical and skew-symmetrical (generalized) loading and displacements.

3.1 Symmetry and skew-symmetry conditions

Symmetric and skew-symmetric loading conditions are mostly relevant for linearly-behaving systems; a nonlinear system may develop an asymmetric response to symmetric loading (e.g. column buckling).

Figure 3.1 collects symmetrical and skew-symmetrical pairs of vectors and moment vectors (moments); those (generalized) vectors are applied at symmetric points in space with respect to the reference plane. Normal and parallel to the plane vectors are considered, that may embody the same named components of a general vector.

The pair members may be moved towards the reference plane up to a vanishing distance ϵ; a point on the reference plane coincides with its image. In the case different (in particular, opposite and nonzero)

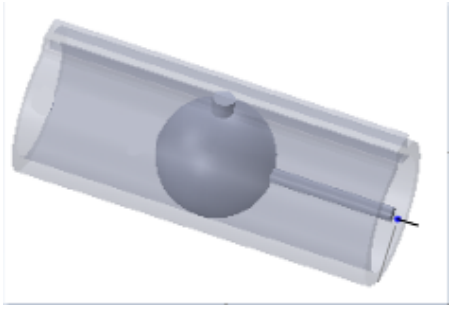

Figure 3.2: The doweled sphere - slotted cylinder joint, which is associated to the skew-symmetry constraint. In this particular application, the cylindrical guide may be considered as grounded.

field vectors are associated to the two coincident pair members, single valuedness does not hold at the reference plane; such condition deserves an attentive rationalization whenever a physical field (displacement field, applied force field, etc.) is to be represented.

Those vector and moment pairs may represent generalized forces (both internal and external) and displacements.

The $*$ (generalized) displacement components may induce material discontinuity at points laying on the [skew-]symmetry plane, if nonzero. They have to be constrained to zero value at those points, thus introducing [skew-]symmetry constraints.

These constraints act in place of the portion of the structure that is omitted from our model, since the results for the whole structure may be derived from the modeled portion alone, due to [skew-]symmetry.

In case of symmetry, a constraint equivalent to a planar joint is to be applied at points laying on the symmetry plane for ensuring displacement/rotation continuity between the modeled portion of the structure, and its image. In case of skew-symmetry, a constraint equivalent to a *doweled sphere - slotted cylinder* joint (see Figure 3.1), where the guide axis is orthogonal to the skew-symmetry plane, is applied at the points belonging to the intersection between the deformable body and the plane.

The $\diamond$ internal action components are null at points pertaining to the [skew-]symmetry plane, since they would otherwise violate the action-reaction law. The complementary $\dagger$ internal action components

are generally nonzero at the [skew-]symmetry plate.

The † external action components are not allowed at points along the [skew-]symmetry plane; instead, the complementary ⋄ generalized force components are allowed, if they are due to external actions.

In the case of a symmetric structure, generally asymmetric applied loads may be decomposed in a symmetric part and in a skew-symmetric part; the problem may be solved by employing a half structure model for both the loadcases; the results may finally be superposed since the system is assumed linear.

3.2 Periodicity conditions

TODO, if needed.

Bibliography

[1] A. E. H. Love, *A treatise on the mathematical theory of elasticity.* Cambridge university press, 2013.